

# AlignGPT: Multi-modal Large Language Models with Adaptive Alignment Capability

Fei Zhao\*, Taotian Pang\*, Chunhui Li, Zhen Wu†, Junjie Guo, Shangyu Xing, Xinyu Dai

National Key Laboratory for Novel Software Technology, Nanjing University

{zhaof, pangtt, lich, guojj, xsy}@smail.nju.edu.cn,

{wuz, daixinyu}@nju.edu.cn

<https://aligngpt-vl.github.io>

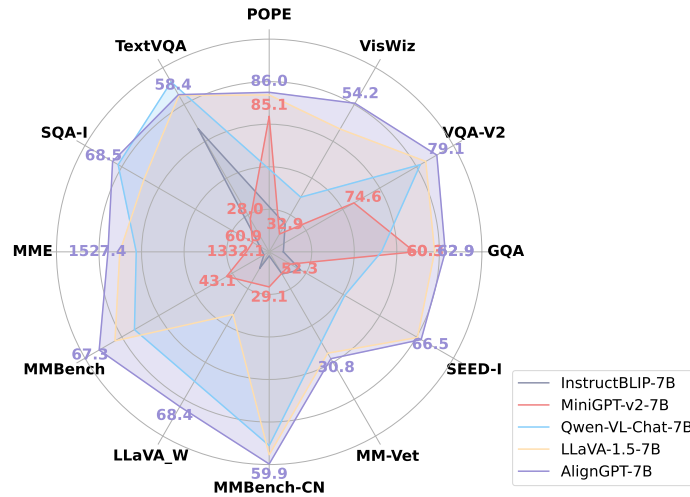


Figure 1: AlignGPT achieves competitive performances on a broad range of vision-language tasks compared with other generalist models. To facilitate observation, we only show the performance of MiniGPT-v2 and AlignGPT. More comprehensive data can be found in Table 1 and Table 2.

## Abstract

Multimodal Large Language Models (MLLMs) are widely regarded as crucial in the exploration of Artificial General Intelligence (AGI). The core of MLLMs lies in their capability to achieve cross-modal alignment. To attain this goal, current MLLMs typically follow a two-phase training paradigm: the pre-training phase and the instruction-tuning phase. Despite their success, there are shortcomings in the modeling of alignment capabilities within these models. Firstly, during the pre-training phase, the model usually assumes that all image-text pairs are uniformly aligned, but in fact the degree of alignment between different image-text pairs is inconsistent. Secondly, the instructions currently used for finetuning incorporate a variety of tasks, different tasks’s instructions usually require different levels of alignment capabilities, but previous MLLMs overlook these differentiated alignment needs. To tackle these issues, we propose a new multimodal large language model AlignGPT. In the pre-training stage, instead of treating all image-text pairs equally, we assign different levels of alignment capabilities to different image-text pairs. Then, in the instruction-tuning phase, we adaptively combine

\*Equal contributions.

†Corresponding author.

these different levels of alignment capabilities to meet the dynamic alignment needs of different instructions. Extensive experimental results show that our model achieves competitive performance on 12 benchmarks.

## 1 Introduction

Multimodal Large Language Models (MLLMs) are considered a crucial step towards achieving Artificial General Intelligence (AGI) [30, 1, 12, 29]. The uniqueness of these models lies in their ability to integrate and understand various types of information, especially text and image data. In the pursuit of AGI, this cross-modal understanding and processing capability is essential, as it mimics how humans interact with the world and comprehend complex information through different senses, such as vision and language. The development of multimodal large language models not only advances the field of artificial intelligence but also provides machines with a way to process and understand information that is closer to human cognition.

Currently, MLLMs typically adhere to a unified training paradigm, which is divided into two key phases: the pre-training phase and the instruction-tuning phase [24, 46, 42, 3, 5, 39, 18, 40, 45]. The pre-training phase concentrates on aligning images with text, aiming to train the model to understand the relevance of image contents and their respective textual descriptions. This alignment imbues the model with cross-modal comprehension abilities. The instruction-tuning phase further enhances its adaptability to specific tasks. This includes enabling the model to complete particular visual-language tasks based on given instructions, such as generating textual descriptions from images, answering questions related to images, or even performing complex reasoning based on both text and images. This training paradigm equips multimodal pre-trained models with not only fundamental cross-modal understanding but also the flexibility to adapt to diverse task demands.

Although current MLLMs have made great progress, the modeling of alignment capabilities during their pre-training and instruction-tuning phases is still insufficient for the following reasons:

- **The degree of alignment is inconsistent between different image-text pairs:** During the pre-training phase, the model typically operates on a key assumption that all image-text pairings are consistently aligned. However, in practical scenarios, the degree of alignment in image-text pairings is not always uniform: in some image-text pairs, the text may describe the whole image while in others the text only describes a part of the image. If these differences are not differentiated during the pre-training phase, it could lead to a misunderstanding of the image-text alignment relationships in the learning process;
- **The instructions for different tasks require different levels of alignment capabilities:** The instructions currently used for finetuning incorporate a variety of tasks. Some of these tasks, like image captioning [41], rely more on global image-text alignment capabilities. In contrast, other tasks, such as visual question answering (VQA) [2], typically require the model to answer questions based on specific parts of the image. This necessitates not only global image-text alignment but also local image-text alignment capabilities. Thus, the instructions of different tasks demand different levels of alignment capabilities.

To effectively enhance the alignment capabilities during the pre-training and instruction-tuning phases, we propose a new multimodal large language model called AlignGPT. In the pre-training phase, we introduce a new paradigm with controllable alignment levels, which does not treat all image-text pairs equally; instead, it assigns different levels of alignment capability to different pairs. This is achieved through CLIP scores [32], where the model categorizes image-text pairs into different alignment levels based on their CLIP scores. A higher alignment level indicates that the text contains more comprehensive information about the image [35, 16]. Subsequently, we utilize these alignment levels as control signals to address the issue of varying degrees of alignment in image-text pairings. During the instruction-tuning phase, we first transform these different levels of alignment capabilities obtained by pre-training into global and local alignment capabilities based on the strength of the alignment levels. Then, we not only assign global alignment capabilities to the instructions of each task, but also adaptively configure different local alignment capabilities according to the alignment needs of each instruction. The broad range of tests conducted demonstrates that our model achieves competitive performance across 12 benchmarks, as shown in Figure 1.

Our contribution can be summarized as follows: (1) We propose a new multi-modal large language model AlignGPT to elevate and empower the alignment capabilities of MLLMs; (2) We propose a novel alignment strategy that generates different levels of alignment capabilities in the pre-training stage, and then adaptively combines these alignment capabilities in the instruction-tuning stage to meet the alignment needs of different instructions; (3) We conduct evaluations across multiple academic benchmarks and multimodal instruction-following benchmarks. Extensive experimental results show that our proposed AlignGPT achieves competitive performance.

## 2 Related Work

In this section, we review the existing studies on large language models and visual language models.

**Large Language Models.** In the field of natural language processing, BERT [10] and GPT-2 [33], as pioneering large pre-trained language models, marked a significant breakthrough in this technological direction. Their training on vast web text datasets demonstrated unprecedented language understanding and generation capabilities. Subsequently, the launch of GPT-3 [4] further accelerated the development of this field, with its large model parameters and extensive training datasets showcasing exceptional abilities in few-shot learning, significantly enhancing task adaptability and flexibility. Following this, the introduction of InstructGPT and ChatGPT [31] focused on optimizing the efficiency and naturalness of interactions between models and humans, where InstructGPT enhanced the capability to execute precise instructions, and ChatGPT improved the conversational experience, making these models more fluent in human-computer communication. Meanwhile, as large language model (LLM) technology continued to evolve, emerging models like LLaMA [38] and GLM [13] began to make their mark. To equip these models with the ability to respond to human instructions similar to ChatGPT, research teams finetune LLaMA and GLM using high-quality instruction datasets, thereby further enhancing its capability to follow instructions, with representative projects such as Alpaca [37], Vicuna [8], and ChatGLM [44].

Although these models have made significant progress in interacting with humans through language, we recognize that human understanding and processing of complex information relies not only on language but also critically on visual and other sensory inputs. The observation has driven us to further explore more comprehensive visual-language models in order to more accurately simulate complex interactions between humans and the real world.

**Visual Language Models.** In recent years, multimodal large language models (MLLMs) have garnered increasing attention. The core of MLLMs lies in their ability to achieve cross-modal understanding and generalization. Most current models, such as LLaVA [24], MiniGPT-4 [46], mPLUG-Owl [42], Qwen-VL [3], MiniGPT-v2 [5], NExT-GPT [40], InternLM-XComposer [45], CogVLM [39], and MM1 [28], utilize a standard training framework consisting of two primary phases: pre-training and instruction-tuning. In the pre-training phase, the model utilizes image caption data to establish a rich understanding of cross-modal semantic knowledge. This training phase enables the model to comprehend and capture the correlation between images and text, establishing a solid foundation for subsequent stage. In the instruction-tuning phase, the model receives specific task instructions to optimize its performance on that task. Through this instruction-tuning phase, the model can further refine its understanding to execute specific tasks, enabling it to flexibly and accurately address various task requirements in practical applications.

Although achieving good results, the current MLLMs overlook two critical factors: first, the degree of alignment between different image-text pairs is inconsistent during the pre-training phase; second, the instructions for different tasks require different levels of alignment capabilities during the instruction-tuning phase. Therefore, the modeling of alignment capabilities in these models remains inadequate. To this end, we propose a new multimodal large language model AlignGPT to effectively enhance the alignment capabilities of MLLMs.

## 3 Methodology

In this section, we initially present the fundamental structure of the visual-language model AlignGPT, followed by a demonstration of how to enhance the alignment capability of the model during both the pre-training and instruction-tuning stages.

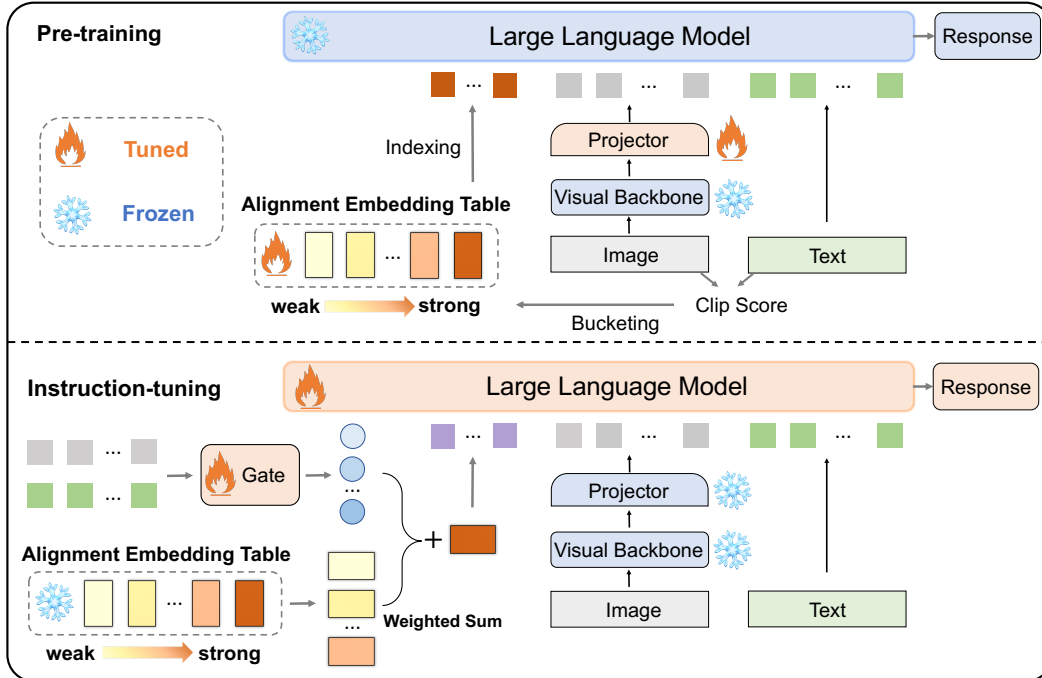


Figure 2: The architecture of AlignGPT.

### 3.1 Architecture

AlignGPT consists of four components: a visual backbone, a linear projection layer, a large language model, and an alignment module. Figure 2 provides an overview of the AlignGPT architecture and its training process. The followings are the implementation details of these components:

**Visual backbone.** We utilize the pre-trained CLIP visual encoder ViT-L/14 [32] as our visual backbone. We train the model using an image resolution of  $336 \times 336$ .

**Linear projection layer.** We adopt a linear projection layer to map the representations of images from the vector space of the vision backbone to that of the language model.

**Large language model.** We choose the open-source model Vicuna [8] as our language model backbone, given its strong ability to follow instructions effectively in various language tasks.

**Alignment module.** We propose to add alignment vectors to the inputs of MLLMs to enrich their alignment capabilities. These alignment vectors are positioned ahead of the image embeddings and text embeddings. In the subsequent sections, we will elaborate on the role of the alignment vectors and the process to acquire them.

### 3.2 Alignment Level-aware Pre-training

As mentioned before, in the pre-training stage, the model usually assumes that all image-text pairs are uniformly aligned, and these pairs are used to train the model to comprehend the relations between images and their corresponding textual descriptions. However, the real-world scenarios show that the degree of alignment between these image-text pairs may vary considerably. Overlooking the difference could lead to a misunderstanding of the image-text alignment relations during the learning process.

Instead of treating all image-text pairs equally, we assign different levels of alignment capabilities to different image-text pairs. To achieve this, we leverage the similarity scores provided by CLIP. The motivation behind this is that CLIP is pre-trained on a large-scale image-text dataset, thus

using CLIP similarity scores to determine alignment levels between images and text is relatively accurate. Image-text pairs with lower CLIP scores suggest that the text describes only part of the image’s information, whereas pairs with higher CLIP scores indicate that the text provides a more comprehensive description of the image [35, 16]. Subsequently, we use these alignment levels as control signals to train the model, enabling it to understand the alignment relations between different image-text pairs.

More precisely, we start by computing the CLIP similarities  $s$  for all training image-text pairs. Then, we rank all image-text pairs based on their similarity scores. Finally, we use a bucketing technique to divide them into  $N$  discrete alignment levels. The process can be represented as:

$$l = \text{bucket}(s), \quad l \in \{1, 2, \dots, N\}, \quad (1)$$

where  $\text{bucket}(\cdot)$  denotes a bucketing function that assigns each pair into one of  $N$  equally spaced intervals and  $l$  is the alignment level of an image-text pair. In this way, image-text pairs with lower CLIP similarity scores are assigned to buckets indicative of lower alignment levels, whereas those with higher CLIP similarity scores are grouped into buckets representing higher alignment levels.

Once the alignment level of each image-text pair is determined, we can regard it as a special token to express the alignment relation between the image and its textual description. This special token is placed ahead of the image and text tokens. During the pre-training phase, in addition to learning the mapping function from the image to the text space in the linear projection layer, we also initialize this special token as an alignment vector and continuously update its representation.

### 3.3 Adaptive Alignment-based Instruction-tuning

Currently, the instructions used for finetuning cover various tasks such as image captioning, visual question answering, and visual grounding, *etc.* The instructions of these tasks place different requirements on the alignment capabilities. For example, image captioning tasks mainly rely on global alignment between images and text, while VQA and visual grounding tasks require not only global alignment but also local alignment capabilities between images and text.

To this end, we first demonstrate how to represent the global and local alignment capabilities between image-text pairs. As mentioned in Section 3.2, after the pre-training stage, we obtain  $N$  alignment vectors  $\{H_1, H_2, \dots, H_N\}$  corresponding to  $N$  discrete alignment levels  $\{1, 2, \dots, N\}$ . Among them,  $H_N$  represents the highest level of alignment, *i.e.*,  $H_N$  indicates that the text provides very comprehensive description of an image. Here we regard it as a global alignment vector. The vectors below  $H_N$  represent different degrees of alignment between the image and the text (*i.e.*,  $\{H_1, H_2, \dots, H_{N-1}\}$ ), which means the text only describes a part of the information of the image from weak to strong. Thus, we regard them as local alignment vectors of varying degrees.

Afterwards, we not only allocate global alignment capabilities to the instructions of each task, but also adaptively distribute varying degrees of local alignment capabilities based on the distinct alignment needs of each instruction. The reason behind this is that global alignment serves as the foundation for cross-modal understanding; only by mastering global alignment capabilities can a model truly focus on enhancing local alignment abilities. Specifically, in addition to the global alignment vectors, we assign different weights to the local alignment vectors via a gate network. These weights are obtained based on input instructions and image, as the input instructions greatly influence the visual regions the model should focus on. The implementation of the gate network is as follows:

$$\alpha = \text{softmax}(W(H_I \otimes H_T) + b), \quad (2)$$

where  $H_I$  and  $H_T$  denote the vector representation of input instruction and image information,  $W$  and  $b$  are weight matrix and bias,  $\alpha$  means the weights of local alignment vectors. Finally, we aggregate the global alignment vector and the local alignment vectors with varying weights to ensure a more precise fulfillment of alignment requirements for each instruction:

$$H_{align} = H_N + \sum_{i=1}^{N-1} \alpha H_i, \quad (3)$$

where  $H_{align}$  means the alignment vector for each instruction during the instruction-tuning stage.

Overall, we can view the alignment vectors obtained during the pre-training phase as foundational components, each with varying alignment capabilities. During the instruction-tuning phase, we dynamically combine these components to meet the alignment needs of different instructions.

Table 1: Performance comparison on multiple academic benchmarks. Res indicates the resolution of the input image. For the baselines, the results with  $\diamond$  are obtained by running the code released by the authors, and the other results are retrieved from [5, 23]. Best results are in bold.

Method	LLM	Res.	Sample Size		VQA <sup>v2</sup>	GQA	VisWiz	SQA <sup>I</sup>	TextVQA
			Pre-train	Finetune					
BLIP-2	Vicuna-13B	224	129M	-	41.0	41.0	19.6	61.0	42.5
InstructBLIP	Vicuna-7B	224	129M	1.2M	-	49.2	34.5	60.5	50.1
InstructBLIP	Vicuna-13B	224	129M	1.2M	-	49.5	33.4	63.1	50.7
Shikra	Vicuna-13B	224	600K	5.5M	77.4	-	-	-	-
IDEFICS-9B	LLaMA-7B	224	353M	1M	50.9	38.4	35.5	-	25.9
IDEFICS-80B	LLaMA-65B	224	353M	1M	60.0	45.2	36.0	-	30.9
MiniGPT-v2	LLaMA2-7B	448	-	-	74.6 $\diamond$	60.3	32.9	60.9 $\diamond$	28.0 $\diamond$
Qwen-VL	Qwen-7B	448	1.4B	50M	78.8	59.3	35.2	67.1	<b>63.8</b>
Qwen-VL-Chat	Qwen-7B	448	1.4B	50M	78.2	57.5	38.9	68.2	61.5
LLaVA-1.5	Vicuna-7B	336	558K	665K	78.5	62.0	50.0	66.8	58.2
LLaVA-1.5	Vicuna-13B	336	558K	665K	<b>80.0</b>	63.3	53.6	<b>71.6</b>	61.3
<b>AlignGPT</b>	Vicuna-7B	336	558K	665K	79.1	62.9	54.2	68.5	58.4
<b>AlignGPT</b>	Vicuna-13B	336	558K	665K	<b>80.0</b>	<b>63.6</b>	<b>56.4</b>	70.3	60.2

Table 2: Results on multimodal instruction-following benchmarks. For the baseline methods, the results on the SEED<sup>I</sup> dataset are obtained from [7], and the other results are retrieved from [23].

Method	LLM	Res.	POPE	MME	MMB	MMB <sup>CN</sup>	SEED <sup>I</sup>	LLaVA <sup>W</sup>	MM-Vet
BLIP-2	Vicuna-13B	224	85.3	1293.8	-	-	46.4	38.1	22.4
InstructBLIP	Vicuna-7B	224	-	-	36.0	23.7	53.4	60.9	26.2
InstructBLIP	Vicuna-13B	224	78.9	1212.8	-	-	-	58.2	25.6
Shikra	Vicuna-13B	224	-	-	58.8	-	-	-	-
IDEFICS-9B	LLaMA-7B	224	-	-	48.2	25.2	-	-	-
IDEFICS-80B	LLaMA-65B	224	-	-	54.5	38.1	-	-	-
MiniGPT-v2	LLaMA2-7B	448	85.1 $\diamond$	1332.1 $\diamond$	43.1 $\diamond$	29.1 $\diamond$	52.3 $\diamond$	-	-
Qwen-VL	Qwen-7B	448	-	-	38.2	7.4	56.3	-	-
Qwen-VL-Chat	Qwen-7B	448	-	1487.5	60.6	56.7	58.2	-	-
LLaVA-1.5	Vicuna-7B	336	85.9	1510.7	64.3	58.3	66.2	63.4	30.5
LLaVA-1.5	Vicuna-13B	336	85.9	1531.3	67.7	63.6	<b>68.2</b>	70.7	35.4
<b>AlignGPT</b>	Vicuna-7B	336	86.0	1527.4	67.3	59.9	66.5	68.4	30.8
<b>AlignGPT</b>	Vicuna-13B	336	<b>86.2</b>	<b>1572.0</b>	<b>69.5</b>	<b>63.7</b>	67.8	<b>75.2</b>	<b>35.6</b>

## 4 Experiments

### 4.1 Experimental Settings

**Datasets.** For a fair comparison, we use the same pre-training and instruction dataset as the LLaVA-1.5 [23]. It mainly includes 558K caption pairs for modality alignment and 665K single- or multi-round conversations for instruction-tuning. Besides, we evaluate AlignGPT on a range of academic visual question answering (VQA) tasks and recent benchmarks designed specifically for MLLMs. This evaluation spans 12 benchmarks, including VQA<sup>V2</sup> [15], GQA [17], VizWiz [17], SQA<sup>I</sup> (ScienceQA-IMG) [27], TextVQA [36], POPE [22], MME [14], MMB (MMBench), MMB<sup>CN</sup> (MMBench-Chinese) [25], SEED<sup>I</sup> (SEED-Bench-IMG) [20], LLaVA<sup>W</sup> (LLaVA-Bench-in-the-Wild) [24], and MM-Vet [43] datasets.

**Implementation Details.** We adopt a ViT [11] model pre-trained with CLIP [32] as a vision encoder to effectively process visual inputs. On the language side, Vicuna [8] is utilized to handle multimodal features, ensuring a cohesive integration of text and visual data. In the pre-training phase, both the visual backbone and the large language model of AlignGPT remain frozen, with only the parameters of the linear projection layer and alignment vectors being trained. During instruction-tuning phase, we freeze the linear projection layer, alignment vectors, and visual backbone, while adjusting the parameters of the large language model and the gate network. The global batch sizes for the two phases are set at 256 and 128 respectively, with DeepSpeed [34] using ZeRO2 and ZeRO3 strategies

Table 3: Influence of different number of alignment level.

Method	Alignment Level	VQA <sup>v2</sup>	GQA	VisWiz	SQA <sup>I</sup>	TextVQA	POPE	MME	MMB	SEED <sup>I</sup>
AlignGPT	Number=4	79.0	62.9	52.3	68.7	58.3	86.2	1463.8	67.2	66.5
AlignGPT	Number=6	79.0	62.7	51.2	68.9	58.3	85.8	1436.3	67.3	66.2
AlignGPT	Number=8	79.1	62.9	54.2	68.5	58.4	86.0	1527.4	67.3	66.5
AlignGPT	Number=10	79.1	62.6	53.0	67.8	58.4	86.2	1481.4	66.4	66.7

Table 4: Influence of local and global alignment.

Settings	Average	Local	Global	VQA <sup>v2</sup>	GQA	VisWiz	SQA <sup>I</sup>	TextVQA	POPE	MME	MMB	SEED <sup>I</sup>
(a)	✗	✓	✗	79.1	62.7	53.3	67.9	58.6	85.9	1467.1	66.9	66.3
(b)	✗	✗	✓	79.1	62.9	52.6	68.3	58.4	85.9	1502.9	66.3	66.2
(c)	✓	✗	✓	79.0	62.8	52.5	68.6	58.4	85.6	1492.5	67.0	66.0
(d)	✗	✓	✓	79.1	62.9	54.2	68.5	58.4	86.0	1527.4	67.3	66.5

accordingly. Regarding our training methodology, we conduct a single epoch of optimization for all models using the AdamW [26] optimizer coupled with a cosine learning schedule. Moreover, we initiate pre-training and instruction-tuning with learning rates of 1e-3 and 2e-5, respectively. The framework is trained on 8 A800 GPUs with 80GB memory.

## 4.2 Compared Methods

We chose a diverse set of representative multimodal large language models (MLLMs) as our baselines, including BLIP-2 [21], InstructBLIP [9], Shikra [6], IDEFICS [19], MiniGPT-v2 [5], Qwen-VL [3], Qwen-VL-Chat [3], and LLaVA-1.5 [23].

## 5 Results and Analysis

### 5.1 Main Results

**Visual Question Answering.** We evaluate AlignGPT using five popular academic benchmarks, as detailed in Table 1. Despite using less training data, the AlignGPT-7B demonstrates competitive performance, surpassing other generalist models including InstructBLIP-13B, Shikra-13B, and IDEFICS-80B on most datasets, except for LLaVA-1.5-13B. These results verify the rationality of the structural design of our model. Moreover, considering that AlignGPT utilizes the same training dataset as LLaVA-1.5, it is evident that AlignGPT-7B outperforms LLaVA-1.5-7B across all evaluation datasets, and AlignGPT-13B also surpasses LLaVA-1.5-13B on the majority of datasets. This demonstrates that our approach has effectively enhance the alignment capabilities of multimodal large language models. The fly in the ointment is that AlignGPT-13B does not perform as well as Qwen-VL on the TextVQA dataset. This may stem from the fact that TextVQA is a text-centric QA task, as it requires identifying text in images to answer questions. AlignGPT is tailored to boost multimodal alignment and might not exhibit strong results in text-focused scenarios.

**MLLM-oriented Multi-modal Benchmarks.** We apply AlignGPT to seven recent popular multi-modal benchmarks, as shown in Table 2. We discover that, apart from LLaVA-1.5-13B, AlignGPT-7B surpassed all previous multimodal models. This shows that our model has strong generalization ability. Additionally, compared to LLaVA-1.5-13B, AlignGPT-13B has shown improvements on most datasets, particularly achieving good advancements on the MME, MMB, and LLaVA<sup>W</sup> benchmarks. This further validates the efficacy of both global and local alignment capabilities.

### 5.2 Ablation Study

Without loss of generality, we choose AlignGPT-7b for the ablation study to investigate the effects of different components.

**Impact of Number of Alignment Levels.** To investigate the effect of the number of alignment levels  $N$  on AlignGPT, we vary the value of  $N$  in the range of [4, 10] with a step size of 2. Table

Table 5: Influence of different input image resolutions.

Method	LLM	Resolution	VQA <sup>v2</sup>	GQA	SQA <sup>I</sup>	TextVQA	POPE	MMB	SEED <sup>I</sup>
AlignGPT	Vicuna-7B	336	79.1	62.9	68.5	58.4	86.0	67.3	66.5
AlignGPT	Vicuna-7B	672	79.7	63.3	68.3	60.3	86.8	67.2	66.5
AlignGPT	Vicuna-7B	1008	79.8	63.4	68.2	60.3	86.8	67.2	66.6

Table 6: Influence of different large language models.

Method	LLM	Resolution	VQA <sup>v2</sup>	GQA	SQA <sup>I</sup>	MME	MMB	MMB <sup>CN</sup>	SEED <sup>I</sup>
AlignGPT	LLaMA2-7B-Chat	336	79.1	62.9	65.9	1500.8	66.6	57.9	66.4
AlignGPT	Vicuna-7B	336	79.1	62.9	68.5	1527.4	67.3	59.9	66.5
AlignGPT	LLaMA3-8B-Base	336	79.6	63.1	70.4	1539.7	72.0	67.7	68.2

3 shows the performance of AlignGPT with different  $N$  on nine datasets. Actually, AlignGPT can achieve good results at  $N = 4$ , and their performance remains stable as the number of alignment levels increases. Depending on the trajectory of the curve, their performance has an initial upward trend and then flattens out. These observations indicate that AlignGPT can improve the alignment capabilities of multi-modal large language models based on a small number of alignment levels. Finally, according to the trend of the curve, we set  $N$  to 8.

**Impact of Local and Global Alignment.** During the instruction-tuning phase, we assign global alignment capabilities and local alignment capabilities to the instructions of each task. Here, we explore the role of separate global alignment capabilities and local alignment capabilities on AlignGPT. Among them, “Local” refers to the local alignment capabilities derived by assigning different weights to various local alignment vectors using a gate network. “Global” denotes the global alignment capabilities, and “Average” represents the local alignment capabilities obtained by assigning equal weights to each local alignment vector. The performance of these four strategies (settings a-d) is presented in Table 4. As we can see, setting(a) and setting(b) demonstrate divergent performances in downstream tasks, which can be attributed to the different demands these tasks place on global and local alignment capabilities. It is worth noting that setting (a) and setting (b) perform worse than our final approach (setting d) on most datasets, which verifies the necessity and superiority of the combination of global and local alignment capabilities. Additionally, the performance of setting (c) is inferior to that of setting (d), a possible reason being that the demands for local alignment capabilities in each downstream task are dynamically variable.

### 5.3 Discussion

**Impact of different input image resolutions.** Image resolution plays a crucial role in vision-language tasks as higher resolutions help reduce image blurring and enhance the understanding of image-text alignment. To evaluate the impact of resolution changes on the performance of multimodal tasks, we increase the image resolution from 336 to 1008, with the resulting performance changes detailed in Table 5. The study results show that higher image resolutions can improve model performance on most multimodal tasks. For example, the score for VQA<sup>v2</sup> increased from 79.1 to 79.8, while the score for TextVQA rose from 58.4 to 60.3. Meanwhile, the performance of the POPE improve by 0.8. These results highlight that appropriately increasing image resolution is an effective strategy for enhancing performance in studies of multimodal large language models.

**Impact of different large language models.** We also explore the impact of the large language model on the performance of AlignGPT, specifically testing three models: LLaMA-2-7B-Chat, Vicuna-v1.5-7B, and the latest LLaMA-3-8B-Base. The results are shown in Table 6. Initially, we observe that LLaMA-3-8B-Base achieves the best performance, followed by Vicuna-v1.5-7B, with LLaMA-2-7B-Chat performing the worst, which is reasonable given LLaMA-3-8B-Base’s larger parameter size and richer training data. Besides, we find that compared to the VQA tasks, Vicuna-v1.5-7B performs better on multimodal benchmarks such as MME, MMB, and SEED<sup>I</sup> than LLaMA-2-7B-Chat, possibly because Vicuna-v1.5-7B underwent supervised instruction-tuning with ShareGPT data, and ShareGPT contains some background knowledge related to downstream tasks.



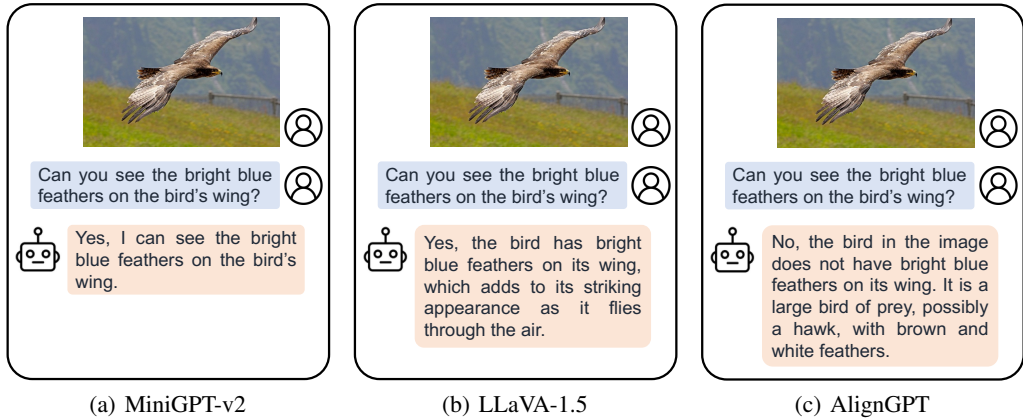


Figure 3: Comparison with other models.

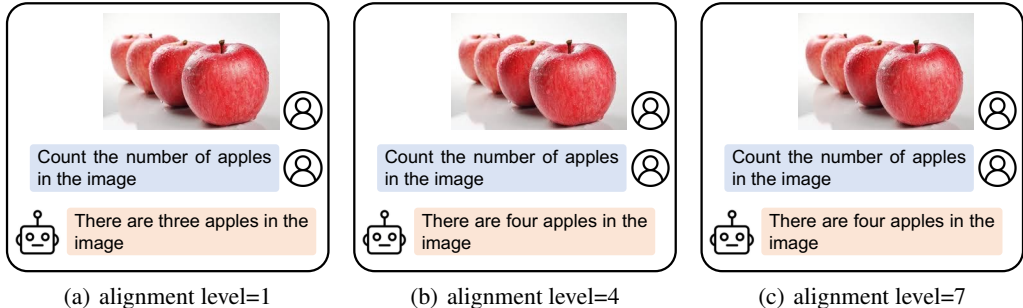


Figure 4: The responses of AlignGPT under different levels of alignment capability.

## 5.4 Qualitative Results

Figure 3 presents a comparative analysis of our model with MiniGPT-v2 [5] and LLaVA-1.5 [23]. When a user submits an image alongside the instruction “Can you see the bright blue feathers on the bird’s wing?”, MiniGPT-v2 and LLaVA-1.5 both return an incorrect answer “Yes”. In contrast, our model produces accurate result “No”, thereby demonstrating that AlignGPT can effectively enhance the model’s alignment capability. In Figure 4, we further demonstrate the responses of AlignGPT under different levels of alignment capability. We find that with lower alignment levels, the model may only focus on certain regions of the image, resulting in an undercount of the total number of apples; whereas with higher alignment levels, the model considers the entire image area, thus achieving accurate apple quantity estimation. This finding once again underscores the necessity of enhancing the alignment capability of MLLMs.

## 6 Conclusion

In this paper, we propose AlignGPT, a novel multimodal large language model designed to bolster the alignment capabilities of MLLMs. Our approach involves utilizing the alignment level of data as a control signal during pre-training to effectively handle the varying degrees of alignment in image-text pairs. Subsequently, in the instruction-tuning phase, we begin by exploiting these control signals to shape different levels of alignment capabilities. Continuing from this, we go beyond assigning global alignment capabilities to instructions of each task; we also dynamically configure distinct local alignment capabilities based on the specific demands of each instruction. Results from numerous experiments indicate that our AlignGPT achieves better performance than other state-of-the-art MLLMs. Further analysis validates the superiority of our AlignGPT.

## References

- [1] Rohan Anil, Sebastian Borgeaud, Yonghui Wu, Jean-Baptiste Alayrac, Jiahui Yu, Radu Soricut, Johan Schalkwyk, Andrew M. Dai, Anja Hauth, Katie Millican, David Silver, Slav Petrov, Melvin Johnson, Ioannis Antonoglou, Julian Schrittwieser, Amelia Glaese, Jilin Chen, Emily Pitler, Timothy P. Lillicrap, Angeliki Lazaridou, Orhan Firat, James Molloy, Michael Isard, Paul Ronald Barham, Tom Hennigan, Benjamin Lee, Fabio Viola, Malcolm Reynolds, Yuanzhong Xu, Ryan Doherty, Eli Collins, Clemens Meyer, Eliza Rutherford, Erica Moreira, Kareem Ayoub, Megha Goel, George Tucker, Enrique Piqueras, Maxim Krikun, Iain Barr, Nikolay Savinov, Ivo Danihelka, Becca Roelofs, Anaïs White, Anders Andreassen, Tamara von Glehn, Lakshman Yagati, Mehran Kazemi, Lucas Gonzalez, Misha Khalman, Jakub Sygnowski, and et al. Gemini: A family of highly capable multimodal models. *CoRR*, abs/2312.11805, 2023.
- [2] Stanislaw Antol, Aishwarya Agrawal, Jiasen Lu, Margaret Mitchell, Dhruv Batra, C. Lawrence Zitnick, and Devi Parikh. VQA: visual question answering. In *2015 IEEE International Conference on Computer Vision, ICCV 2015, Santiago, Chile, December 7-13, 2015*, pages 2425–2433. IEEE Computer Society, 2015.
- [3] Jinze Bai, Shuai Bai, Shusheng Yang, Shijie Wang, Sinan Tan, Peng Wang, Junyang Lin, Chang Zhou, and Jingren Zhou. Qwen-vl: A frontier large vision-language model with versatile abilities. *CoRR*, abs/2308.12966, 2023.
- [4] Tom B. Brown, Benjamin Mann, Nick Ryder, Melanie Subbiah, Jared Kaplan, Prafulla Dhariwal, Arvind Neelakantan, Pranav Shyam, Girish Sastry, Amanda Askell, Sandhini Agarwal, Ariel Herbert-Voss, Gretchen Krueger, Tom Henighan, Rewon Child, Aditya Ramesh, Daniel M. Ziegler, Jeffrey Wu, Clemens Winter, Christopher Hesse, Mark Chen, Eric Sigler, Mateusz Litwin, Scott Gray, Benjamin Chess, Jack Clark, Christopher Berner, Sam McCandlish, Alec Radford, Ilya Sutskever, and Dario Amodei. Language models are few-shot learners. In *Advances in Neural Information Processing Systems 33: Annual Conference on Neural Information Processing Systems 2020, NeurIPS 2020, December 6-12, 2020, virtual*, 2020.
- [5] Jun Chen, Deyao Zhu, Xiaoqian Shen, Xiang Li, Zechun Liu, Pengchuan Zhang, Raghuraman Krishnamoorthi, Vikas Chandra, Yunyang Xiong, and Mohamed Elhoseiny. Minigt-v2: large language model as a unified interface for vision-language multi-task learning. *CoRR*, abs/2310.09478, 2023.
- [6] Keqin Chen, Zhao Zhang, Weili Zeng, Richong Zhang, Feng Zhu, and Rui Zhao. Shikra: Unleashing multimodal llm’s referential dialogue magic. *CoRR*, abs/2306.15195, 2023.
- [7] Lin Chen, Jinsong Li, Xiaoyi Dong, Pan Zhang, Conghui He, Jiaqi Wang, Feng Zhao, and Dahua Lin. Sharegpt4v: Improving large multi-modal models with better captions. *CoRR*, abs/2311.12793, 2023.
- [8] Wei-Lin Chiang, Zhuohan Li, Zi Lin, Ying Sheng, Zhanghao Wu, Hao Zhang, Lianmin Zheng, Siyuan Zhuang, Yonghao Zhuang, Joseph E Gonzalez, et al. Vicuna: An open-source chatbot impressing gpt-4 with 90%\* chatgpt quality. See <https://vicuna.lmsys.org> (accessed 14 April 2023), 2(3):6, 2023.
- [9] Wenliang Dai, Junnan Li, Dongxu Li, Anthony Meng Huat Tiong, Junqi Zhao, Weisheng Wang, Boyang Li, Pascale Fung, and Steven C. H. Hoi. Instructblip: Towards general-purpose vision-language models with instruction tuning. In *Advances in Neural Information Processing Systems 36: Annual Conference on Neural Information Processing Systems 2023, NeurIPS 2023, New Orleans, LA, USA, December 10 - 16, 2023*, 2023.
- [10] Jacob Devlin, Ming-Wei Chang, Kenton Lee, and Kristina Toutanova. BERT: pre-training of deep bidirectional transformers for language understanding. In *Proceedings of the 2019 Conference of the North American Chapter of the Association for Computational Linguistics: Human Language Technologies, NAACL-HLT 2019, Minneapolis, MN, USA, June 2-7, 2019, Volume 1 (Long and Short Papers)*, pages 4171–4186. Association for Computational Linguistics, 2019.

- [11] Alexey Dosovitskiy, Lucas Beyer, Alexander Kolesnikov, Dirk Weissenborn, Xiaohua Zhai, Thomas Unterthiner, Mostafa Dehghani, Matthias Minderer, Georg Heigold, Sylvain Gelly, Jakob Uszkoreit, and Neil Houlsby. An image is worth 16x16 words: Transformers for image recognition at scale. In *International Conference on Learning Representations*, 2021.
- [12] Danny Driess, Fei Xia, Mehdi S. M. Sajjadi, Corey Lynch, Aakanksha Chowdhery, Brian Ichter, Ayzan Wahid, Jonathan Tompson, Quan Vuong, Tianhe Yu, Wenlong Huang, Yevgen Chebotar, Pierre Sermanet, Daniel Duckworth, Sergey Levine, Vincent Vanhoucke, Karol Hausman, Marc Toussaint, Klaus Greff, Andy Zeng, Igor Mordatch, and Pete Florence. Palm-e: An embodied multimodal language model. In Andreas Krause, Emma Brunskill, Kyunghyun Cho, Barbara Engelhardt, Sivan Sabato, and Jonathan Scarlett, editors, *International Conference on Machine Learning, ICML 2023, 23-29 July 2023, Honolulu, Hawaii, USA*, volume 202 of *Proceedings of Machine Learning Research*, pages 8469–8488. PMLR, 2023.
- [13] Zhengxiao Du, Yujie Qian, Xiao Liu, Ming Ding, Jiezhong Qiu, Zhilin Yang, and Jie Tang. Glm: General language model pretraining with autoregressive blank infilling. In *Proceedings of the 60th Annual Meeting of the Association for Computational Linguistics (Volume 1: Long Papers)*, pages 320–335, 2022.
- [14] Chaoyou Fu, Peixian Chen, Yunhang Shen, Yulei Qin, Mengdan Zhang, Xu Lin, Zhenyu Qiu, Wei Lin, Jinrui Yang, Xiawu Zheng, Ke Li, Xing Sun, and Rongrong Ji. MME: A comprehensive evaluation benchmark for multimodal large language models. *CoRR*, abs/2306.13394, 2023.
- [15] Yash Goyal, Tejas Khot, Douglas Summers-Stay, Dhruv Batra, and Devi Parikh. Making the V in VQA matter: Elevating the role of image understanding in visual question answering. In *2017 IEEE Conference on Computer Vision and Pattern Recognition, CVPR 2017, Honolulu, HI, USA, July 21-26, 2017*, pages 6325–6334. IEEE Computer Society, 2017.
- [16] Chanda Grover, Indra Deep Mastan, and Debayan Gupta. Contextclip: Contextual alignment of image-text pairs on CLIP visual representations. In Soma Biswas, Shanmuganathan Raman, and Amit K. Roy-Chowdhury, editors, *Proceedings of the Thirteenth Indian Conference on Computer Vision, Graphics and Image Processing, ICVGIP 2022, Gandhinagar, India, December 8-10, 2022*, pages 51:1–51:10. ACM, 2022.
- [17] Danna Gurari, Qing Li, Abigale J. Stangl, Anhong Guo, Chi Lin, Kristen Grauman, Jiebo Luo, and Jeffrey P. Bigham. Vizwiz grand challenge: Answering visual questions from blind people. In *2018 IEEE Conference on Computer Vision and Pattern Recognition, CVPR 2018, Salt Lake City, UT, USA, June 18-22, 2018*, pages 3608–3617. Computer Vision Foundation / IEEE Computer Society, 2018.
- [18] Wenbo Hu, Yifan Xu, Yi Li, Weiyue Li, Zeyuan Chen, and Zhuowen Tu. BLIVA: A simple multimodal LLM for better handling of text-rich visual questions. In *Thirty-Eighth AAAI Conference on Artificial Intelligence, AAAI 2024, Thirty-Sixth Conference on Innovative Applications of Artificial Intelligence, IAAI 2024, Fourteenth Symposium on Educational Advances in Artificial Intelligence, EAAI 2024, February 20-27, 2024, Vancouver, Canada*, pages 2256–2264. AAAI Press, 2024.
- [19] Hugo Laurençon, Lucile Saulnier, Léo Tronchon, Stas Bekman, Amanpreet Singh, Anton Lozhkov, Thomas Wang, Siddharth Karamcheti, Alexander M. Rush, Douwe Kiela, Matthieu Cord, and Victor Sanh. OBELICS: an open web-scale filtered dataset of interleaved image-text documents. In *Advances in Neural Information Processing Systems 36: Annual Conference on Neural Information Processing Systems 2023, NeurIPS 2023, New Orleans, LA, USA, December 10 - 16, 2023*, 2023.
- [20] Bohao Li, Rui Wang, Guangzhi Wang, Yuying Ge, Yixiao Ge, and Ying Shan. Seed-bench: Benchmarking multimodal llms with generative comprehension. *CoRR*, abs/2307.16125, 2023.
- [21] Junnan Li, Dongxu Li, Silvio Savarese, and Steven C. H. Hoi. BLIP-2: bootstrapping language-image pre-training with frozen image encoders and large language models. In *International Conference on Machine Learning, ICML 2023, 23-29 July 2023, Honolulu, Hawaii, USA*, volume 202 of *Proceedings of Machine Learning Research*, pages 19730–19742. PMLR, 2023.

- [22] Yifan Li, Yifan Du, Kun Zhou, Jinpeng Wang, Wayne Xin Zhao, and Ji-Rong Wen. Evaluating object hallucination in large vision-language models. In *Proceedings of the 2023 Conference on Empirical Methods in Natural Language Processing, EMNLP 2023, Singapore, December 6-10, 2023*, pages 292–305. Association for Computational Linguistics, 2023.
- [23] Haotian Liu, Chunyuan Li, Yuheng Li, and Yong Jae Lee. Improved baselines with visual instruction tuning. *CoRR*, abs/2310.03744, 2023.
- [24] Haotian Liu, Chunyuan Li, Qingyang Wu, and Yong Jae Lee. Visual instruction tuning. In *Advances in Neural Information Processing Systems 36: Annual Conference on Neural Information Processing Systems 2023, NeurIPS 2023, New Orleans, LA, USA, December 10-16, 2023*, 2023.
- [25] Yuan Liu, Haodong Duan, Yuanhan Zhang, Bo Li, Songyang Zhang, Wangbo Zhao, Yike Yuan, Jiaqi Wang, Conghui He, Ziwei Liu, Kai Chen, and Dahua Lin. Mmbench: Is your multi-modal model an all-around player? *CoRR*, abs/2307.06281, 2023.
- [26] Ilya Loshchilov and Frank Hutter. Decoupled weight decay regularization. In *International Conference on Learning Representations*, 2019.
- [27] Pan Lu, Swaroop Mishra, Tanglin Xia, Liang Qiu, Kai-Wei Chang, Song-Chun Zhu, Oyvind Tafjord, Peter Clark, and Ashwin Kalyan. Learn to explain: Multimodal reasoning via thought chains for science question answering. In *Advances in Neural Information Processing Systems 35: Annual Conference on Neural Information Processing Systems 2022, NeurIPS 2022, New Orleans, LA, USA, November 28 - December 9, 2022*, 2022.
- [28] Brandon McKinzie, Zhe Gan, Jean-Philippe Fauconnier, Sam Dodge, Bowen Zhang, Philipp Dufter, Dhruvi Shah, Xianzhi Du, Futang Peng, Floris Weers, Anton Belyi, Haotian Zhang, Karanjeet Singh, Doug Kang, Ankur Jain, Hongyu Hè, Max Schwarzer, Tom Gunter, Xiang Kong, Aonan Zhang, Jianyu Wang, Chong Wang, Nan Du, Tao Lei, Sam Wiseman, Guoli Yin, Mark Lee, Zirui Wang, Ruoming Pang, Peter Grasch, Alexander Toshev, and Yinfei Yang. MM1: methods, analysis & insights from multimodal LLM pre-training. *CoRR*, abs/2403.09611, 2024.
- [29] Seungwhan Moon, Andrea Madotto, Zhaojiang Lin, Tushar Nagarajan, Matt Smith, Shashank Jain, Chun-Fu Yeh, Prakash Murugesan, Peyman Heidari, Yue Liu, Kavya Srinet, Babak Damavandi, and Anuj Kumar. Anymal: An efficient and scalable any-modality augmented language model. *CoRR*, abs/2309.16058, 2023.
- [30] OpenAI. GPT-4 technical report. *CoRR*, abs/2303.08774, 2023.
- [31] Long Ouyang, Jeffrey Wu, Xu Jiang, Diogo Almeida, Carroll L. Wainwright, Pamela Mishkin, Chong Zhang, Sandhini Agarwal, Katarina Slama, Alex Ray, John Schulman, Jacob Hilton, Fraser Kelton, Luke Miller, Maddie Simens, Amanda Askell, Peter Welinder, Paul F. Christiano, Jan Leike, and Ryan Lowe. Training language models to follow instructions with human feedback. In *Advances in Neural Information Processing Systems 35: Annual Conference on Neural Information Processing Systems 2022, NeurIPS 2022, New Orleans, LA, USA, November 28 - December 9, 2022*, 2022.
- [32] Alec Radford, Jong Wook Kim, Chris Hallacy, Aditya Ramesh, Gabriel Goh, Sandhini Agarwal, Girish Sastry, Amanda Askell, Pamela Mishkin, Jack Clark, Gretchen Krueger, and Ilya Sutskever. Learning transferable visual models from natural language supervision. In Marina Meila and Tong Zhang, editors, *Proceedings of the 38th International Conference on Machine Learning, ICML 2021, 18-24 July 2021, Virtual Event*, volume 139 of *Proceedings of Machine Learning Research*, pages 8748–8763. PMLR, 2021.
- [33] Alec Radford, Jeffrey Wu, Rewon Child, David Luan, Dario Amodei, Ilya Sutskever, et al. Language models are unsupervised multitask learners. *OpenAI blog*, 1(8):9, 2019.
- [34] Samyam Rajbhandari, Jeff Rasley, Olatunji Ruwase, and Yuxiong He. Zero: memory optimizations toward training trillion parameter models. In *Proceedings of the International Conference for High Performance Computing, Networking, Storage and Analysis, SC 2020, Virtual Event / Atlanta, Georgia, USA, November 9-19, 2020*, page 20. IEEE/ACM, 2020.

- [35] Christoph Schuhmann, Richard Vencu, Romain Beaumont, Robert Kaczmarczyk, Clayton Mullis, Aarush Katta, Theo Coombes, Jenia Jitsev, and Aran Komatsuzaki. LAION-400M: open dataset of clip-filtered 400 million image-text pairs. *CoRR*, abs/2111.02114, 2021.
- [36] Amanpreet Singh, Vivek Natarajan, Meet Shah, Yu Jiang, Xinlei Chen, Dhruv Batra, Devi Parikh, and Marcus Rohrbach. Towards VQA models that can read. In *IEEE Conference on Computer Vision and Pattern Recognition, CVPR 2019, Long Beach, CA, USA, June 16-20, 2019*, pages 8317–8326. Computer Vision Foundation / IEEE, 2019.
- [37] Rohan Taori, Ishaan Gulrajani, Tianyi Zhang, Yann Dubois, Xuechen Li, Carlos Guestrin, Percy Liang, and Tatsunori B Hashimoto. Alpaca: A strong, replicable instruction-following model. *Stanford Center for Research on Foundation Models*. <https://crfm.stanford.edu/2023/03/13/alpaca.html>, 3(6):7, 2023.
- [38] Hugo Touvron, Thibaut Lavril, Gautier Izacard, Xavier Martinet, Marie-Anne Lachaux, Timothée Lacroix, Baptiste Rozière, Naman Goyal, Eric Hambro, Faisal Azhar, Aurélien Rodriguez, Armand Joulin, Edouard Grave, and Guillaume Lample. Llama: Open and efficient foundation language models. *CoRR*, abs/2302.13971, 2023.
- [39] Weihang Wang, Qingsong Lv, Wenmeng Yu, Wenyi Hong, Ji Qi, Yan Wang, Junhui Ji, Zhuoyi Yang, Lei Zhao, Xixuan Song, Jiazheng Xu, Bin Xu, Juanzi Li, Yuxiao Dong, Ming Ding, and Jie Tang. Cogvlm: Visual expert for pretrained language models. *CoRR*, abs/2311.03079, 2023.
- [40] Shengqiong Wu, Hao Fei, Leigang Qu, Wei Ji, and Tat-Seng Chua. Next-gpt: Any-to-any multimodal LLM. *CoRR*, abs/2309.05519, 2023.
- [41] Kelvin Xu, Jimmy Ba, Ryan Kiros, Kyunghyun Cho, Aaron C. Courville, Ruslan Salakhutdinov, Richard S. Zemel, and Yoshua Bengio. Show, attend and tell: Neural image caption generation with visual attention. In Francis R. Bach and David M. Blei, editors, *Proceedings of the 32nd International Conference on Machine Learning, ICML 2015, Lille, France, 6-11 July 2015*, volume 37 of *JMLR Workshop and Conference Proceedings*, pages 2048–2057. JMLR.org, 2015.
- [42] Qinghao Ye, Haiyang Xu, Guohai Xu, Jiabo Ye, Ming Yan, Yiyang Zhou, Junyang Wang, Anwen Hu, Pengcheng Shi, Yaya Shi, Chenliang Li, Yuanhong Xu, Hehong Chen, Junfeng Tian, Qian Qi, Ji Zhang, and Fei Huang. mplug-owl: Modularization empowers large language models with multimodality. *CoRR*, abs/2304.14178, 2023.
- [43] Weihao Yu, Zhengyuan Yang, Linjie Li, Jianfeng Wang, Kevin Lin, Zicheng Liu, Xinchao Wang, and Lijuan Wang. Mm-vet: Evaluating large multimodal models for integrated capabilities. *CoRR*, abs/2308.02490, 2023.
- [44] Aohan Zeng, Xiao Liu, Zhengxiao Du, Zihan Wang, Hanyu Lai, Ming Ding, Zhuoyi Yang, Yifan Xu, Wendi Zheng, Xiao Xia, Weng Lam Tam, Zixuan Ma, Yufei Xue, Jidong Zhai, Wenguang Chen, Zhiyuan Liu, Peng Zhang, Yuxiao Dong, and Jie Tang. GLM-130B: an open bilingual pre-trained model. In *The Eleventh International Conference on Learning Representations, ICLR 2023, Kigali, Rwanda, May 1-5, 2023*. OpenReview.net, 2023.
- [45] Pan Zhang, Xiaoyi Dong, Bin Wang, Yuhang Cao, Chao Xu, Linke Ouyang, Zhiyuan Zhao, Shuangrui Ding, Songyang Zhang, Haodong Duan, Wenwei Zhang, Hang Yan, Xinyue Zhang, Wei Li, Jingwen Li, Kai Chen, Conghui He, Xingcheng Zhang, Yu Qiao, Dahua Lin, and Jiaqi Wang. Internlm-xcomposer: A vision-language large model for advanced text-image comprehension and composition. *CoRR*, abs/2309.15112, 2023.
- [46] Deyao Zhu, Jun Chen, Xiaoqian Shen, Xiang Li, and Mohamed Elhoseiny. Minigpt-4: Enhancing vision-language understanding with advanced large language models. *CoRR*, abs/2304.10592, 2023.